EuroIntervention

First-In-Man application of a miniature self-contained intracoronary magnetic resonance probe.
A multi-centre safety and feasibility trial

E. Regar[1]*, B. Hennen[2], E. Grube[3], D. Halon[4], R.L. Wilensky[5], R. Virmani[6], J. Schneiderman[7], S. Sax[8], H. Friedmann[8], P.W. Serruys[1], W. Wijns[9]

1. Department of Interventional Cardiology, Thoraxcenter, Erasmus Medical Center, Rotterdam, The Netherlands; 2. Staedtisches Krankenhaus Pirmasens, Germany; 3. Heart Center, Siegburg, Germany; 4. Carmel Medical Center, Haifa, Israel; 5. Cardiovascular Division, Hospital of the University of Pennsylvania, Philadelphia, USA; 6. CVPath, International Registry of Pathology, Gaithersburg, MD 20878, USA; 7. The Department of Vascular Surgery, and the Gottesdiener Vascular Biology Laboratory, The Sackler Faculty of Medicine Tel Aviv University, Tel Aviv, Israel; 8. TopSpin Medical (Israel) Ltd., Global Park, 2 Yodfat St, Lod, Israel; 9. Cardiovascular Center, Aalst, Belgium

KEYWORDS

Intravascular MR, plaque characterization, coronary artery

Abstract

Aims: To assess safety and feasibility of intracoronary Magnetic Resonance (MR) Spectroscopy in living patients, using a self-contained MR catheter.

Methods and results: Prospective, multi-centre study in patients with stable or unstable angina that were scheduled for percutaneous coronary diagnostic or therapeutic catheterization. We assessed the feasibility of an intravascular MR catheter, capable of analysing the arterial wall without external magnets or coils, by differentiating lipid rich, intermediate and fibrotic areas of the atherosclerotic plaque on the basis of differential water diffusion.

Twenty-nine patients were included at 4 centres. The intracoronary MR-spectroscopy procedure was well tolerated; no MACE and no device related serious adverse event was observed. The MR catheter was successfully advanced into the lesion in 28 patients. Introduction of the MR catheter was not possible in one patient with a tortuous proximal right coronary artery. MR data were obtained in 22 patients. According to the predominant MR pattern, lesions were classified as fibrous plaque in 4 patients, as intermediate plaque in 4 patients and as lipid-rich plaque in 8 patients. Six patients were excluded from analysis because artifacts impeded the quality of the MR signal. Plaque type did not show a correlation with angina status (p=0.552; all groups) or angiographic parameters, such as minimal lumen diameter and diameter stenosis.

Conclusions: This prospective, multi-centre study demonstrates for the first time that coronary artery assessment of potentially vulnerable, non-flow limiting lesions using a dedicated intravascular MR catheter, free of external magnets or coils, is feasible in clinical practice. Assessment of the coronary wall may provide important data regarding the composition of the atherosclerotic lesion, which then could contribute to predicting the likelihood of eventual rupture and clinical instability.

* Corresponding author: Thoraxcenter Ba 585, Dr. Molewaterplein 40, 3015 GD Rotterdamn, The Netherlands
E-mail: e.regar@erasmusmc.nl

Introduction

Acute coronary events are caused in the majority of cases by coronary lesions with the propensity of rupture or erosion resulting in acute thrombosis. These lesions do not necessarily present as haemodynamically significant prior to the acute clinical event. Non-flow limiting lesions are made ubiquitous by coronary angiography and Multislice Computed Tomography but they are missed by non-invasive functional diagnostic approaches. Therefore, for non-flow limiting stenoses, prevention of acute coronary syndromes relies on the detection of plaque which is prone to rupture, causing coronary thrombosis.

Postmortem studies revealed several types of plaques that are at high risk to rupture. A prominent role is being assigned to the thin fibrous cap atheroma (TCFA). It is defined by a large lipid core, a thin fibrous cap and increased macrophage infiltration. Similarly, in-vivo intravascular ultrasound imaging and angioscopic observations support the role of lipid rich plaque for subsequent coronary events. Magnetic resonance (MR) can provide detailed tissue characterization of atherosclerotic plaques. However, it is difficult to apply MR Spectroscopy to coronary lesions due to cardiac motion caused by myocardial contraction and respiration. The approach presented in this paper is novel and differs fundamentally from conventional MR with or without intravascular coils.

A self-contained intravascular MR (IVMR) probe was designed to obtain high-resolution MR. A recent experimental study confirmed that catheter-based IVMR Spectroscopy can identify fibrous and lipid-rich tissue by measuring differential water diffusion in postmortem aorta samples and coronary arteries[11].

The current study was performed to evaluate the safety and feasibility of this novel intracoronary MR catheter in living patients.

Methods

Study design

Prospective, multicentre, open-label, observational study.

Patients

The patient cohort consisted of individuals with stable or unstable angina that were scheduled for percutaneous coronary diagnostic or therapeutic catheterization. Patients with post-infarct angina (Braunwald class IIIC), acute or chronic renal failure, or any other severe systemic disease were excluded. Intravascular MR Spectroscopy acquisition was performed in a native coronary artery in a short (less than 20 mm in length), non-flow limiting lesion (defined as ≤50% diameter stenosis) with no planned intervention. Arteries with evidence of thrombus, marked calcification or tortuousity, narrow lesions with a minimal lumen diameter less than 2 mm, occluded vessels and saphenous bypass grafts were excluded. The study protocol was approved by the local ethical committee and all patients have given written informed consent.

IVMR analysis

Intravascular MR system. The intravascular MR analysis (IVMR) system has been described in detail elsewhere. In brief, it consists of a self contained, 5.2 F IVMR catheter (Figure 1), a catheter inter-
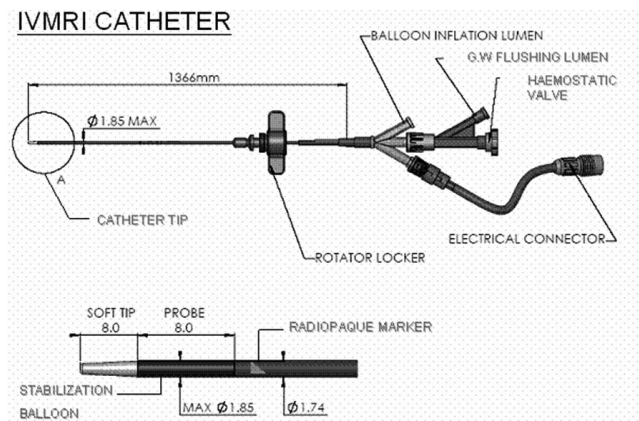

Figure 1. Schematic of the intravascular MR catheter. The catheter has an outer diameter of (5.2F). The intravascular MR probe as well as the side balloon for stabilization is located at the tip of the catheter. The catheter is introduced into the artery in over-the-wire technique via a central lumen.

face unit (CIU), and an external control/display console (TopSpin Medical Ltd., Lod, Israel) (Figure 2).

Intravascular MR Spectroscopy principles of operations. The technology is based on a self contained intravascular MR probe located at the tip of an intravascular catheter. The probe is characterized by strong static magnetic field gradients, in which self-diffusion of the excited spins is the dominant spin relaxation mechanism. A diffusion-weighted signal is measured from the interrogated voxel using a Carr-Purcell-Meiboom-Gill (CPMG) pulse train. CPMG is a MR acquisition method with 90° phase shift in the rotating frame of reference between the 90° pulse and the subsequent 180° pulses to reduce accumulating effects of imperfections in the 180° pulses due to non-homogeneity of the field.

The signal decay is dependent upon self-diffusion of water molecules present in the tissues that make up the artery wall. In fibrous tissue, diffusion of water molecules in the extracellular matrix of the intima is not significantly restricted, resulting in an apparent diffusion coefficient (ADC) which is close to that of freely diffusing water. In the presence of lipids (e.g., cholesterol and cholesterol ester in
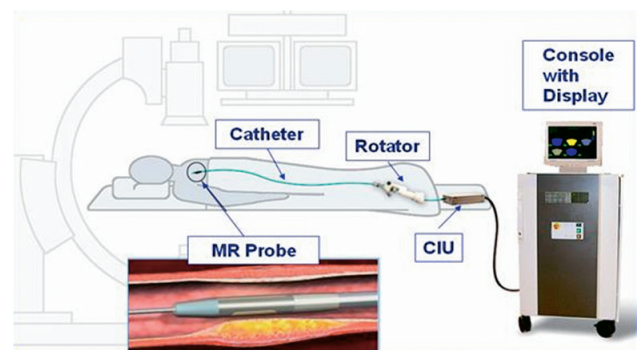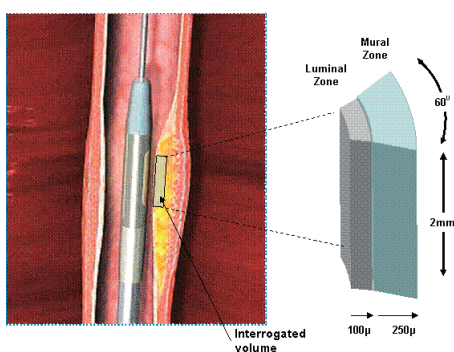

Figure 2. Schematic representation of the intravascular MR Spectroscopy system. It consists of a self contained IVMR catheter, a rotator for manipulation of the catheter tip, a catheter interface unit (CIU), and an external control/display console (Topspin Medical Ltd., Lod, Israel)

the necrotic core or foam cells) diffusion becomes hindered, as the small water molecules need to diffuse between the large-radii lipid molecules, giving rise to ADC, which is significantly lower than that of fibrous tissue.

The spin echo decay curve is characterized by a time constant, inversely proportional to ADC. A lipid fraction index (LFI) is generated from the spin-echo decay curve where fibrous tissue (large ADC, short decay) corresponds to low LFI values, while lipid-rich tissues (small ADC, long decay) correspond to high LFI values.

IVMR data acquisition. The magnetic fields generated by the probe located at the tip of the catheter[13], create a sector-shaped field of view (FOV) looking sideways into the artery wall. The FOV is a 60° sector in the angular plane (lateral resolution), 2.0 mm in the longitudinal plane (slice thickness) and up to 250 µm in the radial plane (depth into the vessel wall). IVMR spectra are averaged for 2 separate zones: a superficial, 0 to 100 µm luminal zone; and a deeper, 100-250 µm mural zone (Figure 3). The signal acquisition time is 51 seconds per FOV.

Figure 3. Schematic representation of the IVMR data acquisition. The magnetic fields generated by the probe located at the tip of the catheter, create a sector-shaped field of view (FOV) looking sideways into the artery wall. The FOV is a 60° sector in the angular plane (lateral resolution), 2.0 mm in the longitudinal plane (slice thickness) and up to 250 µm in the radial plane (depth into the vessel wall). Within this FOV, IVMR assessment is performed simultaneously in 2 separate zones: a superficial, luminal 0 to 100 µm zone and a deeper 100-250 µm zone. A side balloon stabilizes the MR probe against the vessel wall.

The subsequent data readout based on reconstruction done by the spectrometer is instantaneous. Acquired data for each zone within the FOV are displayed as color-coded sectors. Color-coding of the IVMR signals is based on the LFI of the sample volume, where blue indicates no lipids and yellow, a high lipid content.

IVMR data stratification. Postmortem studies have shown that lipid fraction corresponds to histological tissue composition. Based on previous data obtained from an ex-vivo model in human aortas lesions were classified according to the predominant IVMR pattern as fibrous plaque (<30% LFI), intermediate plaque (31-55% LFI) and lipid-rich plaque (>55% LFI).

IVMR Spectroscopy procedure. For the IVMR procedure, the standard femoral approach was used. The IVMR catheter was introduced through an 8F guiding catheter placed in the coronary artery orifice and advanced in over-the wire technique into the target lesion. To achieve high resolution imaging the IVMR catheter was stabilized vis-a-vis the arterial wall by a low-pressure inflation (1.0 atm, ~60 seconds) of a partially occlusive side-balloon and IVMR measurement in one sector was obtained. The balloon was deflated and the probe rotated by using a manual rotation device in fixed increments of 120° to provide additional measurements. A total of 3 sequential inflation/deflation cycles was performed per lesion.

Concomitant medication

All patients were on chronic therapy with acetylsalicylic acid (100 mg daily) and received unfractionated heparin to achieve an activated clotting time > 300 s during the procedure. Intracoronary nitrates – isosorbide dinitrate (ISDN) or glyceryl trinitrate (NTG) according to the local standard – were administered prior to the introduction of the IVMR catheter in order to avoid vasospasm during imaging. Other medication was left to the discretion of the operator.

Angiographic analysis

All angiograms were evaluated after intracoronary administration of nitrates using commercially available software for quantitative coronary angiography. The minimal lumen diameter (MLD) and the reference diameter (RD) at the site of MLD were determined on-site by the investigators. No central analysis of the angiograms was performed. The diameter stenosis (DS) was calculated from the MLD and RD.

Study end-points

Primary study endpoint. The system safety was assessed as primary endpoint and was defined as absence of MACE at 30 days follow-up. MACE was defined as a composite of cardiac death, myocardial infarction (Q wave and non-Q wave), unstable angina or sub-acute thrombosis of the interrogated coronary artery.

Secondary study endpoints were defined as device success, incidence in rise in CK-MB (above upper limit of normal at 12 to 24 hours post-procedure), and incidence of dissection, no-reflow, acute closure and perforation in the interrogated coronary artery.

Device success was defined as ability to position the catheter across the target lesion, to receive a signal from the vessel wall, to perform 3 rotations of the catheter and three successful balloon inflation/deflations.

Follow-up

Clinical follow-up was performed at 24h and 30d after the procedure and included angina status, laboratory testing (CK, CK-MB) and ECG. Throughout the study, any adverse event was collected and monitored until adequately resolved or explained.

Statistical analysis

Numerical data are presented as mean ± SD unless otherwise noted. An unpaired t-test was used to determine significant differences and a p value of <0.05 was considered statistically significant.

Results

Patients

A total of 29 patients of which 5 presented with unstable angina were included. Patient demographic and angiographic data are given in Table 1. The patient cohort showed typical age, gender and cardiovascular risk factor distribution.

MR analysis success

The IVMR catheter was successfully advanced into the lesion in 28/29 patients. Introduction of the IVMR catheter was not possible in one patient with a tortuous proximal right coronary artery. In 27/28 patients all three MR data acquisition cycles were completed. An example of clinical data acquisition is given in Figure 4.
IV MR data were detected in 22/28 interrogated lesions. However, in 6/22 lesions the MR signal quality was impeded by artifacts. These data were excluded from further analysis. Reasons for IVMR failure were artifacts caused by the guide wire or interference by ECG in the catheterization laboratory, and low signal due to insufficient adherence of the IVMR probe to the vessel wall or calcium deposition.
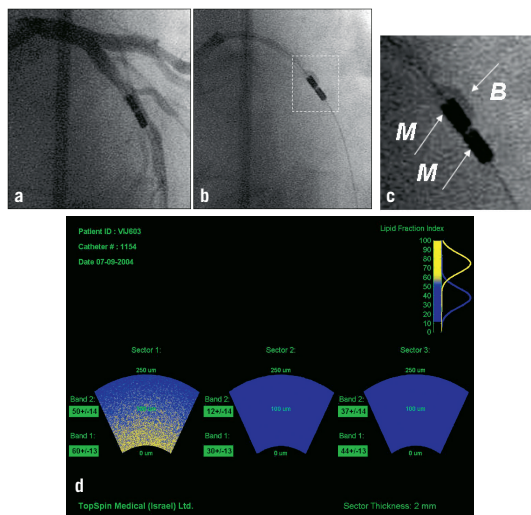

Figure 4. Clinical example of intracoronary IVMR imaging. a. Coronary angiogram of the LAD. b. Position of in intravascular MR catheter in the target lesion. The inflated side balloon hampers the distal flow of x-ray contrast. c. Magnification shows the 2 radiopaque magnets at the distal catheter tip (M) and the inflated side balloon (B). d. Color-coded display of the obtained intravascular MR data. The obtained sectors are blue, indicative for fibrous plaque.

IVMR findings

Lesions with optimal MR quality were classified according to the predominant IVMR pattern: in 4 patients as fibrous plaque, in another 4 as intermediate plaque, and as lipid-rich plaque in 8 patients. The lipid fraction and ADC values as well as angiographic lesion characteristics for the observed plaque types are summarized in Table 2. IVMR derived plaque type did not show a correlation with angina status (p=0.552, all groups) or minimal lumen diameter and diameter stenosis (Figure 5). A comparison of the LFI distribution in our patient cohort with data obtained in postmortem aortas and coronary arteries is given in Figure 6.

Table 1. Patient and lesion characteristics, n = 29

	Patients n (%)
Male	23 (79)
Age (years)	66±12
Angina status	
Stable angina	17
Unstable angina	5
Silent ischaemia	7
Cardiovascular Risk Factors	
Current smoking	5 (17)
Diabetes	7 (24)
IDDM	3
NIDDM	4
Hypertension	23 (79)
Dyslipidaemia	20 (69)
Positive family history of CAD	13 (45)
Cardiac history	
Q wave MI	3 (10)
Non-Q wave MI	4 (14)
Prior CABG	1 (3)
Prior PCI	8 (28)
LVEF (%)	60.42±18.62
Target vessel	
RCA	11
LAD	14
LCX	4
RD (mm)	3.52±0.6
MLD (mm)	2.53±0.64
DS (%)	26.3±13.4
Lesion length (mm)	11.63±8.33
Lesion type	
A	21
B1	8
Morphology	
Concentric	24
Eccentric	5
Thrombus	0
Calcification	1
TIMI flow	
Baseline	3
Post -procedure	3
Multi-vessel disease	21

|	
IDDM	insulin dependent diabetes mellitus
NIDDM	non-insulin dependent diabetes mellitus
CAD	coronary artery disease
MI	myocardial infarction
CABG	coronary artery bypass graft
PCI	percutaneous coronary intervention
LVEF	left ventricular ejection fraction
RCA	right coronary artery
LAD	left anterior descending coronary artery
LCx	left circumflex artery
RD	reference diameter
MLD	minimal lumen diameter
DS	diameter stenosis

5a

5b
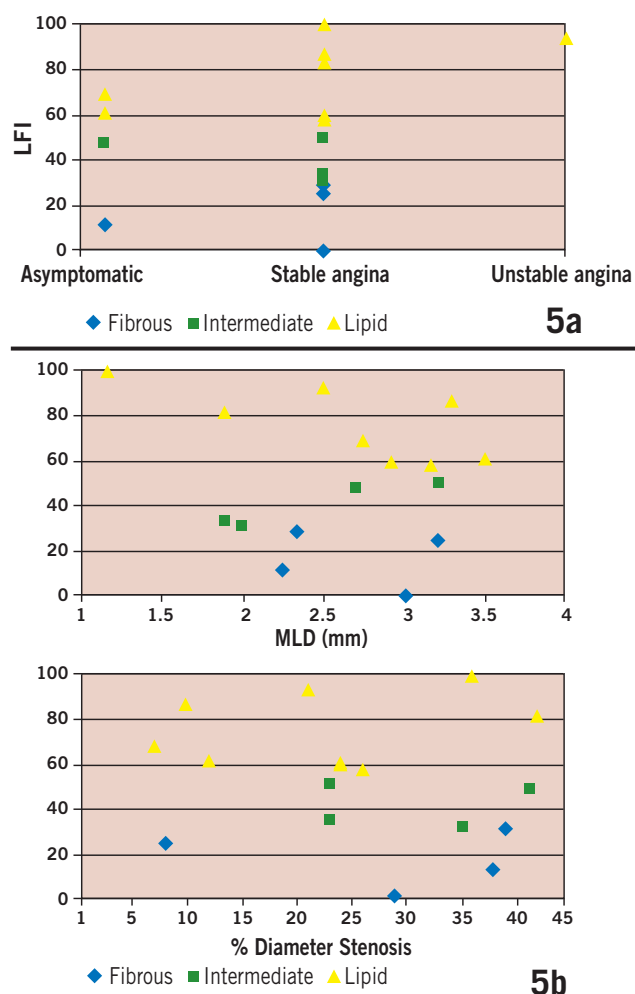
Figure 5. Intravascular MR derived plaque types vs. clinical presentation and angiographic parameters of lesion severity (n=16 subgroup with optimal IV MR data quality)
(a) Frequency distribution of fibrous, intermediate and lipid-rich plaques in patients presenting with unstable angina, stable angina and asymptomatic.
(b) Intravascular MR derived plaque types vs. angiographic minimal lumen diameter (MLD; upper portion) and diameter stenosis (lower portion).

Procedural safety and follow-up

The IVMR Spectroscopy procedure was safe and well tolerated. Transient ECG changes (ST-segment elevation) during inflation of the side balloon were observed in 10/28 patients. In one patient IVMR data acquisition was interrupted after completion of 2 sectors because of ischaemia that resolved immediately after deflation of the side balloon. No MACE was observed. There was no occurrence of spasm, dissection, acute closure or perforation. In-hospital course was uneventful in all patients. All patients completed 30 days follow-up. There was no MACE throughout the complete duration of the study (Table 3).
Two non-device related serious adverse events requiring hospital admission were reported. One patient with coronary multivessel disease and insulin-dependent diabetes mellitus experienced on day 29 a hypoglycemic syncope accompanied by an episode of chest

Table 2. Intravascular MR-derived plaque classification based on ADC, LFI and angiography lesion characteristics.
N = 16 (subgroup with optimal IVMR data quality)

	Fibrous plaque (n=4)	Intermediate plaque (n=4)	Lipid plaque (n=8)
IVMR Spectroscopy			
ADC ($10e^{-9}n2s^{-1}$)	1.6±0.4	0.8±0.2	0.6±0.1
LFI	16.3±13.3	40.8±9.6	76.4±16.4
Angiography			
Target vessel			
RCA	2	1	2
LAD	1	3	5
LCX	1	0	1
RD (mm)	3.79±0.32	3.80±0.73	3.39±0.72
MLD (mm)	2.70±0.48	2.45±0.63	2.65±0.79
DS (%)	28.50±14.39	30.50±9.00	22.25±12.45
Lesion length (mm)	10.75±14.17	12.30±7.17	13.13±7.49
Lesion type			
A	4	2	6
B1	0	2	2
Morphology			
Concentric	3	4	6
Eccentric	1	0	2
Thrombus	0	0	0
Calcification	0	0	0
TIMI flow			
Baseline	3	3	3
Post procedure	3	3	3
Multi-vessel disease	3	3	6

ADC   Apparent diffusion coefficient
LFI   Lipid fraction index

Table 3. Major adverse clinical events within the follow-up period of 30 days (n = 29)

	Patients (n)
Event	
Cardiac death	0
Acute MI	0
New unstable angina	0
Subacute thrombosis	0

pain and a mild rise in cardiac enzymes (CK 438 IU/l, CK-MB 86 IU/l; normal values CK <174 IU/l, CK-MB <24 IU/l or < 6% CK). Coronary angiography, however, was unchanged with respect to the index procedure. Another patient was readmitted at day 29 with atypical chest pain. Ischaemia was excluded by laboratory, ECG and stress tests. Coronary angiogram was unchanged with respect to the index procedure.

Discussion

We are reporting for the first time the coronary application of a novel, dedicated, intravascular MR catheter, free of external magnets or coils, in clinical practice.
This "First-in-Man" study was focused on safety and performance of the IVMR catheter system and Spectroscopy procedure. Our
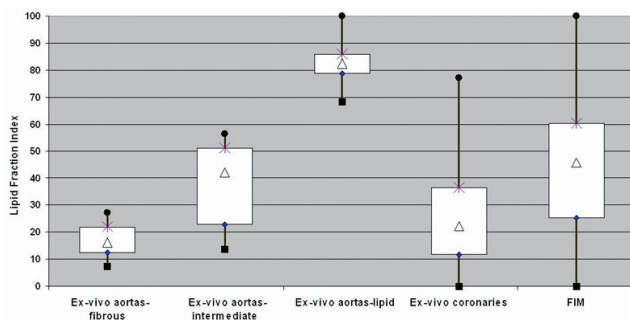
Figure 6. Box-plot presentation of the lipid fraction index (LFI) across preclinical and clinical studies (n=16 subgroup with optimal IV MR data quality) with the IVMR system.

main findings are (1) intracoronary IVMR Spectroscopy using a dedicated catheter is feasible and safe in selected cases; (2) *in-vivo* MR data shows a wide range of lipid fraction indexes, corresponding to different degrees of lipid contents in coronary plaques.

The approach presented in this paper is novel and differs fundamentally from conventional MRI with or without intravascular coils. It lessons important limitations involved in conventional MRI techniques that are based on creating the magnetic fields from outside the patient. One of these is the relative motion of coronary arteries with respect to gradient fields that limits the spatial resolution. In addition, using large and expensive MRI scanners in dedicated MRI laboratories limits their use during interventional procedures.

Using a standard interventional approach the above described intravascular MR catheter was successfully advanced into the target lesion in 28/29 (97%) of cases. This success rate is high considering that 7 imaged lesions had a relatively narrow lumen diameter of < 2mm by QCA.

Our intravascular MR observations in living patients, which are in accordance to previously reported postmortem findings, show a wide range of lipid fraction indexes. A comparison of lipid fraction indexes diagnosed in postmortem coronary arteries, in postmortem aortas and our in-vivo findings is illustrated in Figure 6. This analysis confirms that a wide spectrum of lipid fraction indexes can be diagnosed in atherosclerotic human arteries, despite obvious differences in the samples and methods.

Based on the *in-vitro* validation algorithms, lipid fraction index was translated into a clinically meaningful classification ranging from fibrotic plaque (low lipid fraction index), to intermediate plaque (intermediate lipid fraction index), to lipid-rich plaques (high lipid fraction index). Our intravascular MR-derived plaque classification did not correlate with classical angiographic parameters for lesion severity. This is in accordance with previous studies showing that coronary angiography is only a fair predictor of subsequent coronary events. The percentage diameter stenosis of a lesion does not provide reliable information regarding the risk for myocardial infarction and death. A possible explanation is the systematic angiographic underestimation of plaque extent, and the inability to distinguish between stable and unstable plaques.

The unique information of intravascular derived MR plaque characterization could enhance the arsenal of invasive diagnostic techniques, such as angioscopy, intravascular ultrasound, palpography and optical coherence tomography that focus on different features of TCFA.

Limitations and future developments

This study was designed to test feasibility of a newly developed IVMR catheter in the clinical setting. Accordingly, a number of technical issues became apparent and triggered further engineering improvements during the duration of the study. Obvious limitations of the current IVMR catheter are its size (5.2F), the susceptibility to electromagnetic noise, and in some cases insufficient adherence of the IVMR probe to the vessel wall. Proper apposition of the IVMR catheter to the vessel wall is achieved by inflating a balloon within the artery, which impedes coronary blood flow. The duration of data acquisition (51 sec per sector) makes it difficult to scan multiple lesions. Although not observed in our patient cohort, it cannot completely be excluded that balloon inflation might carry a risk of damaging the arterial wall. This might be particularly problematic at a site that is suspected to be vulnerable due to high lipid content and thinned fibrous cap.

Intravascular MR using this probe is not a reflection of the actual morphology of the plaque, but provides a simplified spatial representation of its lipid-rich component as a two-dimensional sector. One possibility for scanning the vessel circumference is to turn the catheter within the lesion in such a way that sequentially different sectors of the coronary artery segment are being imaged. Precise rotation of the distal catheter tip was difficult. Limited rotational accuracy and relatively sparse sampling of the vessel wall with the current MR probe prevents complete interrogation of the plaque, leaving blind spots that may contain vulnerable areas.

Recent histopathology data evaluating the circumferential distribution of the necrotic core of TCFA's has shown that vulnerable plaques have an angular span of at least 120° in over 75% of the cases. Therefore it may not be mandatory to sample 360° of vessel circumference to diagnose TCFA. In any case, further development is anticipated to enable scanning of the complete vessel circumference during longitudinal catheter pullback and alleviate the need for acquiring individual sectors.

Success rate of Intracoronary IVMR Spectroscopy procedure was 76% (22/29 patients) in the clinical setting. This was lower than expected from previous preclinical trials. Electromagnetic interference was caused by certain instrumentation in the catheterization laboratory such as ECG and guidewires. In these cases ECG was replaced with IVMR compatible equipment and operators restricted to use specific, approved guide wires.

Low signal to noise ratio (SNR) values were encountered in most of the mural zone as well as some of the luminal zone measurements. In consequence, the software has been changed to measure only a modified mural zone. As a result the SNR of the mural zone increased by a factor of $\sqrt{2}$.

This observation is important as it underlines the need for small scale, human feasibility trials when developing innovative invasive technologies. The problems faced were specifically related to equipment in a clinical catheterization laboratory and not observed during the extensive preclinical testing.

Currently, a new generation of IVMR catheters is under development with smaller probe diameters that are compatible with low-profile guide catheters, increased FOV per sensor and multiple-sensors for increasing the number of data points per measurement. These improved IVMR catheters have been developed to address some of the limitations of the current design and will be available for larger scale clinical trials.

We demonstrate here for the first time that coronary artery assessment of potentially vulnerable, non flow-limiting lesions using a dedicated intravascular MR catheter, free of external magnets or coils, is feasible in clinical practice. Assessment of the coronary wall may provide important data regarding the composition of the atherosclerotic lesion, and thereby may contribute to predicting the likelihood of eventual rupture and clinical instability.

References

1. Virmani R, Burke AP, Farb A. Plaque rupture and plaque erosion. *Thromb Haemos.* 1999;82 Suppl 1:1-3.

2. Fuster V, Badimon L, Badimon JJ, Chesebro JH. The pathogenesis of coronary artery disease and the acute coronary syndromes (2). *N Engl J Med.* 1992;326:310-318.

3. Falk E. Plaque rupture with severe pre-existing stenosis precipitating coronary thrombosis. Characteristics of coronary atherosclerotic plaques underlying fatal occlusive thrombi. *Br Heart J.* 1983;50:127-134.

4. Lee RT, Libby P. The unstable atheroma. *Arterioscler Thromb Vasc Biol.* 1997;17:1859-1867.

5. Ambrose JA, Tannenbaum MA, Alexopoulos D, Hjemdahl-Monsen CE, Leavy J, Weiss M, Borrico S, Gorlin R, Fuster V. Angiographic progression of coronary artery disease and the development of myocardial infarction. *J Am Coll Cardiol.* 1988;12:56-62.

6. Schaar JA, Muller JE, Falk E, Virmani R, Fuster V, Serruys PW, Colombo A, Stefanadis C, Ward Casscells S, Moreno PR, Maseri A, van der Steen AF. Terminology for high-risk and vulnerable coronary artery plaques. Report of a meeting on the vulnerable plaque, June 17 and 18, 2003, Santorini, Greece. *Eur Heart J.* 2004;25:1077-1082.

7. Yamagishi M, Terashima M, Awano K, Kijima M, Nakatani S, Daikoku S, Ito K, Yasumura Y, Miyatake K. Morphology of vulnerable coronary plaque: insights from follow-up of patients examined by intravascular ultrasound before an acute coronary syndrome. *J Am Coll Cardiol.* 2000;35:106-111.

8. Uchida Y, Nakamura F, Tomaru T, Morita T, Oshima T, Sasaki T, Morizuki S, Hirose J. Prediction of acute coronary syndromes by percutaneous coronary angioscopy in patients with stable angina. *Am Heart J.* 1995;130:195-203.

9. Danias PG, Roussakis A, Ioannidis JP. Diagnostic performance of coronary magnetic resonance angiography as compared against conventional X-ray angiography: a meta-analysis. *J Am Coll Cardiol.* 2004;44:1867-1876.

10. Schneiderman J, Wilensky RL, Weiss A, Samouha E, Muchnik L, Chen-Zion M, Ilovitch M, Golan E, Blank A, Flugelman M, Rozenman Y, Virmani R. Diagnosis of thin-cap fibroatheromas by a self-contained intravascular magnetic resonance imaging probe in ex vivo human aortas and in situ coronary arteries. *J Am Coll Cardiol.* 2005;45:1961-1969.

11. Blankenhorn D. Coronary arterial calcification. *Am J Med Sci.* 1961;7:41-49.

12. Zur Y. An algorithm to calculate the NMR signal of a multi spin-echo sequence with relaxation and spin-diffusion. *J Magn Reson.* 2004;17:97-106.

13. Wilensky R, Song H, Ferrari V. Role of magnetic resonance in the detection of vulnerable plaques. *J Am Coll Cardiol.* 2006; in press.

14. Koktzoglou I, Simonetti O, Li D. Coronary artery wall imaging: initial experience at 3 Tesla. *J Magn Reson Imaging.* 2005;21:128-132.

15. Holmes DR Jr, Davis K, Gersh BJ, Mock MB, Pettinger MB. Risk factor profiles of patients with sudden cardiac death and death from other cardiac causes: a report from the Coronary Artery Surgery Study (CASS). *J Am Coll Cardiol.* 1989;13:524-530.

16. Little WC, Constantinescu M, Applegate RJ, Kutcher MA, Burrows MT, Kahl FR, Santamore WP. Can coronary angiography predict the site of a subsequent myocardial infarction in patients with mild-to-moderate coronary artery disease? *Circulation.* 1988;78:1157-1166.

17. Vlodaver Z, Frech R, Van Tassel RA, Edwards JE. Correlation of the antemortem coronary arteriogram and the postmortem specimen. *Circulation.* 1973;47:162-169.

18. de Servi S, Mazzone A, Ricevuti G, Mazzucchelli I, Fossati G, Angoli L, Valentini P, Boschetti E, Specchia G. Expression of neutrophil and monocyte CD11B/CD18 adhesion molecules at different sites of the coronary tree in unstable angina pectoris. *Am J Cardiol.* 1996;78:564-568.

19. Gurses-Ozden R, Ishikawa H, Hoh ST, Liebmann JM, Mistlberger A, Greenfield DS, Dou HL, Ritch R. Increasing sampling density improves reproducibility of optical coherence tomography measurements. *J Glaucoma.* 1999;8:238-241.

20. Nair A, Kuban BD, Tuzcu EM, Schoenhagen P, Nissen SE, Vince DG. Coronary Plaque Classification With Intravascular Ultrasound Radiofrequency Data Analysis. *Circulation.* 2002;106:2200-2206.

21. Regar E, Schaar J, McFadden EP, van der Giessen WJ, van Mieghem C, Rodriguez-Granillo G, de Jaegere PPT, Serruys PW. Real-time, high resolution optical coherence tomography (OCT) –a potential tool to detect features of vulnerable plaque *in-vivo*? *Eur Heart J.* 2005:3677 (abstract).

22. Huang D, Swanson EA, Lin CP, Schuman JS, Stinson WG, Chang W, Hee MR, Flotte T, Gregory K, Puliafito CA. Optical coherence tomography. *Science.* 1991;254:1178-1181.

23. Schaar J, Regar E, Mastik F, Saia F, De Korte CL, De Feyter PJ, van der Steen AFW, Serruys PW. Incidence of vulnerable plaques in humans: assessment with intravascular palpography. *Eur Heart J.* 2003;24, suppl:P2210 (abstract).

24. Schaar JA, Regar E, Mastik F, McFadden EP, Saia F, Disco C, de Korte CL, de Feyter PJ, van der Steen AF, Serruys PW. Incidence of High-Strain Patterns in Human Coronary Arteries. Assessment With Three-Dimensional Intravascular Palpography and Correlation With Clinical Presentation. *Circulation.* 2004;109:2716-9.

25. MacNeill BD, Jang IK, Bouma BE, Iftimia N, Takano M, Yabushita H, Shishkov M, Kauffman CR, Houser SL, Aretz HT, DeJoseph D, Halpern EF, Tearney GJ. Focal and multi-focal plaque macrophage distributions in patients with acute and stable presentations of coronary artery disease. *J Am Coll Cardiol.* 2004;44:972-979.

26. Jang I, MacNeill B, Yabushita H, *et al. In-Vivo* Visualization of Coronary Plaques in Patients with Non-ST Elevation Myocardial Infarction/Unstable Angina Using Optical Coherence Tomography. *Circulation.* 2002; abstract 3239.

27. Kolodgie FD, Virmani R, Burke AP, Farb A, Weber DK, Kutys R, Finn AV, Gold HK. Pathologic assessment of the vulnerable human coronary plaque. *Heart.* 2004;90:1385-1391.